

Taming Hot CF₃ Radicals: Incrementally Tuned Families of Polyarene Electron Acceptors for Air-Stable Molecular Optoelectronics**

Igor V. Kuvychko,* Karlee P. Castro, S. H. M. Deng, Xue-Bin Wang,* Steven H. Strauss,* and Olga V. Boltalina*

The renaissance in the synthesis of small organic molecules with strong electron-accepting properties, that is, organic semiconductors (OSCs), during the past decade has been spurred by the global economic need for: 1) renewable sources of energy and 2) more-efficient and less-expensive electronic devices that preferably include earth-abundant elements. The replacement of silicon- and metal-based electronic components with rationally designed, finely tuned organic molecules and molecular assemblies should lead to lower weight, flexible, yet robust electronic components and thus provide sustainable, lower cost solutions to many 21st century technological problems. Significant progress in this endeavor requires a deep understanding of the fundamental relationships between molecular structure, solid-state morphology, and electronic and other physicochemical properties of OSCs.

The presence of electron-withdrawing groups (e.g., halogen atoms, cyanide, perfluoroalkyl (R_F), or perfluoroaryl groups) in polycyclic aromatic hydrocarbons (PAHs) results in molecules with enhanced electron-acceptor properties, better air stability, and improved solid-state charge-carrier mobilities.^[1] In particular, organic transistors made with the few available PAH acceptors that bear perfluoroalkyl (PFA) groups have long-term air stability, which can be correlated with either low LUMO energies (ca. −4 eV; estimated by cyclic voltammetry),^[2] or with DFT-predicted gas-phase electron affinities (EAs) above 2.8 eV (believed to be the

threshold value for *n*-channel-device air stability).^[3] The synthetic methods used in the past to prepare PAHs with one or more R_F substituents include: 1) bottom-up design involving multistep coupling reactions of smaller precursors already bearing an R_F group,^[4] 2) metal-catalyzed reactions in solution for modification of PAH intermediates that have reactive substituents such as Cl or Br atoms, intermediates that are themselves not commercially available,^[4b,5] and 3) direct perfluoroalkylation of PAHs.^[6] However, the latter method has not been extensively studied, possibly because of the low yields and poor regioselectivities reported.^[6a,b]

Herein, we have developed a generic, one-step, solvent-, catalyst-, and promoter-free perfluoroalkylation method for the preparation of PAH(CF₃)_{*n*} strong electron acceptors that is potentially applicable to any thermally stable PAH precursor. The method involves a one-pot reaction between the PAH precursor and gaseous CF₃I at elevated temperature, and results in the addition of multiple CF₃ groups to the PAH core by the replacement of H atoms. Reactions of 17 different precursors each provided up to four PAH(CF₃)_{*n*} compositions as the predominant products, in some cases with up to four isomers of particular compositions. The method appears to be truly general: we have prepared, isolated in pure form as single isomers, and studied PAH(CF₃)_{*n*} compounds for seven PAHs, that is, ANTH, AZUL, PENT, PERY, PHEN, PYRN, and TRPH (see Figure 1 and Table 1 for abbreviations), and preliminary results indicate that the method also works for fluorene, fluoranthene, naphthalene, and tetracene as well as for PAHs containing heteroatoms, such as phenazine, phenanthroline, phenothiazine, iminodibenzyl, and perylene-3,4,9,10-tetracarboxylic dianhydride. The reaction mechanism probably involves the formation of “hot” CF₃ radicals by thermally induced dissociation of CF₃I, removal of a PAH H atom by a CF₃ radical to form CHF₃ and a PAH radical, and subsequent reaction of another CF₃ radical with the transient PAH radical to form the new PAH–CF₃ bond.^[7] This sequence would occur *n* times for a given PAH(CF₃)_{*n*} derivative. In one reaction, CHF₃ was identified as one of the products along with I₂ and the PAH(CF₃)_{*n*} derivatives. Numbering schemes for six PAHs are shown in Figure 1 as well as X-ray structures of five of the compounds.

With one exception, we have not yet endeavored to optimize reaction conditions as far as overall yield or product selectivity is concerned. Instead, our two goals were: 1) to demonstrate that families of PAH(CF₃)_{*n*} derivatives could be readily prepared in pure form as single isomers in a single reaction from a variety of parent PAHs and 2) to examine the electronic properties and solid-state morphologies of as many of the new compounds as possible. Therefore, most reactions

[*] Dr. I. V. Kuvychko, K. P. Castro, Prof. S. H. Strauss, Dr. O. V. Boltalina
Department of Chemistry, Colorado State University
Fort Collins, CO 80523 (USA)
E-mail: igor.kuvychko@gmail.com
steven.strauss@colostate.edu
olga.boltalina@colostate.edu

S. H. M. Deng, Dr. X.-B. Wang
Chemical & Materials Sciences Division, Pacific Northwest
National Laboratory
902 Battelle Boulevard, P.O. Box 999, MS K8-88, Richland, WA
99352 (USA)
E-mail: xuebin.wang@pnnl.gov

[**] We thank the U.S. NSF (CHE-1012468 (SHS/OVB) and the Colorado State University Research Foundation for generous support. The PES work was supported by the U.S. Department of Energy (DOE), Division of Chemical Sciences, Geosciences and Biosciences, Office of Basic Energy Sciences and was performed at the EMSL, a national scientific user facility sponsored by DOE's Office of Biological and Environmental Research and located at Pacific Northwest National Laboratory, which is operated for DOE by Battelle.

Supporting information for this article is available on the WWW under <http://dx.doi.org/10.1002/anie.201300085>.

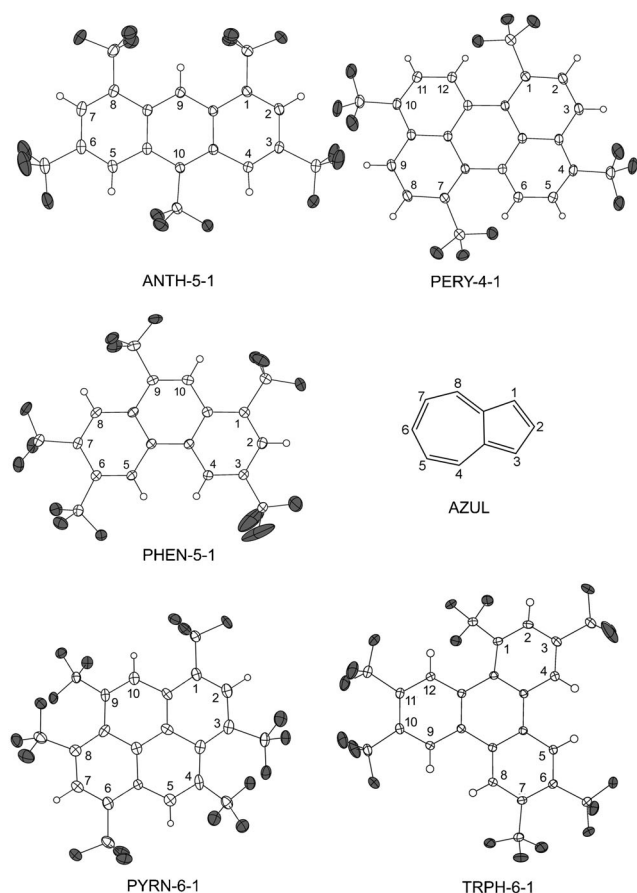


Figure 1. Single-crystal X-ray diffraction ORTEP representations of five compounds listed in Table 1 showing IUPAC locants (thermal ellipsoids are shown at 50% probability except for H atoms, which are spheres of arbitrary size; F atoms are gray).^[12] Also shown are the IUPAC locants for azulene (AZUL). ANTH=Anthracene ($C_{14}H_{10}$), AZUL=azulene ($C_{10}H_8$), PERY=perylene ($C_{20}H_{12}$), PHEN=phenanthrene ($C_{14}H_{10}$), PYRN=pyrene ($C_{16}H_{10}$), TRPH=triphenylene ($C_{18}H_{12}$).

were carried out using only 0.10–0.12 mmol of the PAH precursor (see the Supporting Information, Table S1). We performed a series of reactions starting with 1.0 mmol (178 mg) portions of ANTH that were shown to produce, predominantly, nearly quantitatively, and reproducibly, mixtures of ANTH(CF_3)₄, ANTH(CF_3)₅, and ANTH(CF_3)₆. Isolated yields of the two products obtained after purification by HPLC were 5 mol% for ANTH-5-1 (greater than 95% purity) and 20 mol% ANTH-6-1 (greater than 98% purity; based on ANTH).

Table 1 lists EAs and $E_{1/2}$ values for the new PAH(CF_3)_n compounds. The former were determined by low-temperature photoelectron spectroscopy^[8] and the latter by CV. Also listed are the EAs of the parent PAHs that are reported in the NIST WebBook^[9] and their $E_{1/2}$ values; we determined the latter by using the same apparatus, electrodes, electrolyte, and conditions used for the PAH(CF_3)_n compounds. Representative photoelectron spectra and cyclic voltammograms are shown in Figure 2. The PAH(CF_3)_n EAs range from 1.95(1) eV for PHEN-5-1 to 3.32(2) eV for the mixture of PENT(CF_3)₈ isomers. In contrast, the highest EA for the eight parent

PAHs shown in Table 1 is 1.39(4) eV for PENT; all others are less than 1 eV. The $E_{1/2}$ values range from $-1.73(2)$ V vs. $Fe(Cp)_2^{+/0}$ for TRPH-6-1 to $-0.73(2)$ V for AZUL-5-1, whereas the least negative PAH $E_{1/2}$ value is $-2.14(2)$ V for AZUL; the others range from $-2.23(2)$ V for PERY to less than (i.e., more negative than) -3 V for NAPH, PHEN, and TRPH. A plot of $E_{1/2}$ versus EA for all but three of the entries in Table 1 is shown in Figure 2d. The plot is nominally linear with a slope of 0.73 V eV^{-1} . This finding demonstrates, for a broad set of PAHs and PAH(CF_3)_n derivatives, that an incremental change in $E_{1/2}$ from one compound to the next is, on average, attenuated by 27% relative to the change in EA from one compound to the next. This correlation will be useful for the design of new electron acceptors with targeted EAs, because reduction potentials are much easier to measure than precise values of gas-phase electron affinities. Significantly, the 0.73 V eV^{-1} slope is in contrast to the 1.0 V eV^{-1} slope for a similar plot for aromatic hydrocarbons reported by Ruoff et al. in 1994^[10] (i.e., a 1:1 correlation between $E_{1/2}$ and gas-phase EA for PAHs and PAH derivatives with multiple CF_3 groups was not confirmed in our work; the correlation observed is 0.73:1).

Our EA results also show that there is a nearly linear incremental, and therefore predictable, change in EA for each CF_3 added to PERY, ANTH, and PYRN. A plot of EA versus the number of CF_3 groups is shown in Figure 2b for PERY(CF_3)_n derivatives ($n=0, 4, 5$ (four isomers), 6, and 7). The

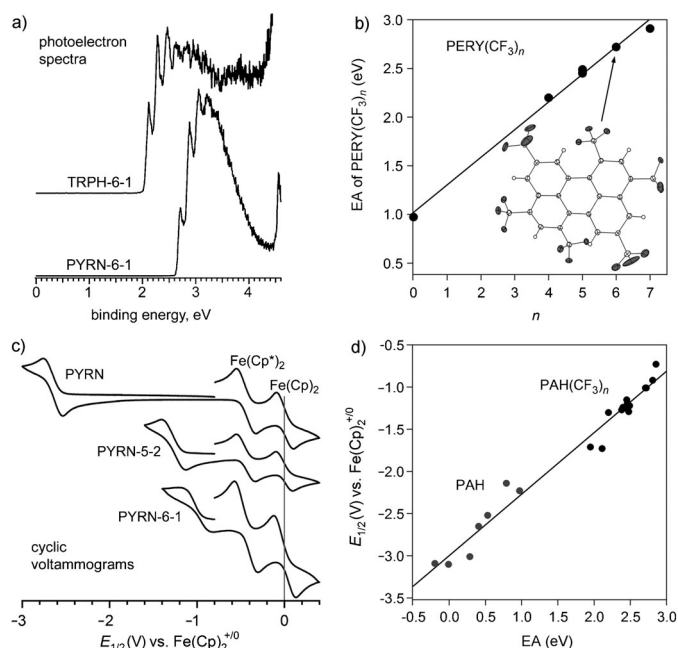


Figure 2. a) Negative-ion photoelectron spectra (12 K, 266 nm) and c) cyclic voltammograms (0.1 M $N(Bu)_4ClO_4$ in dimethoxyethane, 500 mVs^{-1}) of representative PAH(CF_3)_n compounds. b) Plot of PES-determined gas-phase EA of perylene (PERY; $n=0$) and PERY(CF_3)_n compounds ($n=4, 5, 6, 7$) versus the number of CF_3 groups (n). The slope of the least-squares fit to the data is $0.28 \text{ eV per } CF_3 \text{ group}$. d) Plot of $E_{1/2}$ versus gas-phase EA for PAH and PAH(CF_3)_n compounds. The slope of the least-squares fit to the data is 0.73 V eV^{-1} . For both plots, the experimental uncertainties for the PAH(CF_3)_n compounds ($\leq 0.02 \text{ V}$ or 0.02 eV) are smaller than the width of the data points.

Table 1: Experimental results.^[a]

Compound	Abbreviation	Purity [mol %] ^[b]	Yield [mol %]	Gas-Phase EA ^[c] [eV]	$E_{1/2}^{[d]}$ [V] vs. $\text{Fe}(\text{Cp})_2^{+/0}$
anthracene	ANTH	99	—	0.53(2) ^[e]	−2.52
1,3,6,8,10-ANTH(CF ₃) ₅ ^[f]	ANTH-5-1	95	5	2.40(2)	−1.24
2,3,6,7,9,10-ANTH(CF ₃) ₆ ^[g]	ANTH-6-1	98	20	2.81(2)	−0.92
azulene	AZUL	99	—	0.790(8) ^[e]	−2.14
1,2,3,5,7-AZUL(CF ₃) ₅ ^[g]	AZUL-5-1	98	25	2.890(5)	−0.73
naphthalene	NAPH	99	—	−0.2 ^[e]	−3.09
pentacene	PENT	99	—	1.39(4) ^[e]	— ^[h]
PENT(CF ₃) ₈	PENT-8	mixture of isomers	< 2	3.32(2)	— ^[i]
perylene	PERY	99	—	0.973(5) ^[e]	−2.23
1,4,7,10-PERY(CF ₃) ₄ ^[f]	PERY-4-1	98	< 3	2.20(2)	−1.30
1,3,6,8,10-PERY(CF ₃) ₅ ^[f]	PERY-5-1	98	< 3	2.46(2)	−1.19
PERY(CF ₃) ₅	PERY-5-2	95	< 3	2.48(2)	−1.29
PERY(CF ₃) ₅	PERY-5-3	95	< 3	2.49(2)	−1.22
PERY(CF ₃) ₅	PERY-5-4	90	< 3	2.45(2)	−1.15
1,3,5,7,9,11-PERY(CF ₃) ₆ ^[f]	PERY-6-1	97	< 3	2.72(2)	−1.01
PERY(CF ₃) ₇	PERY-7	mixture of isomers	< 2	2.91(2)	— ^[i]
phenanthrene	PHEN	98	—	0.04 ^[e]	−3.10
1,3,6,7,9-PHEN(CF ₃) ₅ ^[f]	PHEN-5-1	95	< 5	1.95(1)	−1.71
pyrene	PYRN	98	—	0.41(1) ^[e]	−2.65
1,3,4,6,8-PYRN(CF ₃) ₅ ^[f]	PYRN-5-1	95	< 3	2.44(2)	−1.25
1,3,4,6,9-PYRN(CF ₃) ₅ ^[g]	PYRN-5-2	70	< 3	2.38(2)	−1.27
1,3,4,6,8,9-PYRN(CF ₃) ₆ ^[g]	PYRN-6-1	95	< 3	2.71(2)	−1.01
triphenylene	TRPH	98	—	0.285(8) ^[e]	−3.01
1,3,6,7,10,11-TRPH(CF ₃) ₆ ^[f]	TRPH-6-1	98	25	2.11(2)	−1.73

[a] All data was obtained by us unless otherwise noted. [b] The purity was determined based on the ¹H and ¹⁹F NMR spectroscopy, NI-APCI mass spectrometry, and HPLC analysis, see the Supporting Information. For commercial samples of starting materials the purity given by vendor is reported.

[c] EA = electron affinity; uncertainty in the least significant digit shown in parentheses. [d] Cyclic voltammetry (CV); anaerobic; 0.1 M N(nBu)₄ClO₄ in dimethoxyethane; platinum working and counter electrodes; silver wire quasi-reference electrode; 500 mVs^{−1}; ferrocene (Fe(Cp)₂) and decamethylferrocene internal standards. [e] Values taken from NIST WebBook; see the Supporting Information for primary references. [f] X-ray structure was obtained and a crystallographic information file (CIF) has been deposited with the Cambridge Structural Database. [g] A preliminary X-ray structure has been determined and the addition pattern and solid-state packing are known but higher-quality data sets will be recorded before CIF files are deposited. If an unsubstituted PAH X-ray structure is known, the reference is listed in the Supporting Information. [h] Insolubility in DME for CV. [i] Mixture of isomers; not measured. NAPH = naphthalene (C₁₀H₈), PHEN = phenanthrene (C₁₄H₁₀). Note that the generic abbreviation PAH(CF₃)_n denotes a compound with *n* H atoms replaced by *n* CF₃ groups (e.g., the composition of ANTH(CF₃)₆ is C₁₄H₈(CF₃)₆, not C₁₄H₁₀(CF₃)₆).

slope of this plot is 0.28 eV per CF₃ group. For ANTH(CF₃)_n and PYRN(CF₃)_n, which have fewer C atoms than PERY(CF₃)_n, the slopes of the corresponding plots are 0.38 and 0.39 eV per CF₃ group, respectively (see the Supporting Information). The slope for the ANTH(CF₃)_n plot of our data is similar to the DFT-predicted slope of 0.35 eV per CF₃ group that was recently reported by Sun et al.^[1e] In that work, the hypothetical isomer chosen for ANTH(CF₃)₆ is coincidentally the same as our new compound ANTH-6-1 (there is also good agreement between Sun's DFT-predicted EA for this compound, 2.73 eV, and the experimental value reported here, 2.81(2) eV). Note that the first prediction of a linear plot of DFT-predicted EA versus number of CF₃ groups was for C₂₀H_{10−n}(CF₃)_n derivatives (C₂₀H₁₀ = corannulene; the reported slope is 0.20 eV per CF₃).^[7]

The X-ray structures reported here reveal two interesting findings that are potentially relevant to the use of PAH(CF₃)_n

derivatives for optoelectronic applications. The first feature is that the number of CF₃ groups attached to ANTH can significantly affect the extent to which neighboring molecules interact through their π clouds. A comparison of neighboring pairs of molecules of ANTH-5-1 and ANTH-6-1 is shown in Figure 3. Note that the molecules are offset differently along both the long and short molecular axes (i.e., the pitch and roll, respectively, are different).^[11] The difference in slippage along the long axis, ca. 0.6 Å for ANTH-5-1 and ca. 4.0 Å for ANTH-6-1, is far greater than that along the short axis. Note that the long axis of the aromatic core is 7.3 Å for ANTH, so the pitch distance in ANTH-6-1 is more than half a molecule.

The second structural feature is that the isomers PYRN-5-1 and PYRN-5-2, which have nearly identical EAs and $E_{1/2}$ values and have four of their five CF₃ groups in common positions, have very different relative orientations between neighboring molecules in their respective lattices (Figure 3). This difference leads to significant differences in π – π stacking. In PYRN-5-1, the aromatic cores of neighboring molecules are essentially parallel but are rotated 45° with respect to one another, resulting in the near superposition of three rings in each molecule. In PYRN-5-2, on the other hand, the closest parallel neighboring aromatic cores are not rotated, have essentially zero roll

distance, and have a pitch distance equivalent to one half of the distance between *para*-C atoms on the hexagonal rings, resulting in a significantly offset stacking geometry.

Finally, we have measured the air stability in the presence of bright light and the fluorescence quantum yields for selected compounds (see the Supporting Information). The results described here demonstrate that our generic synthetic method, coupled with highly efficient HPLC purification, could be used to make many dozens of new PAH(R_F)_n compounds, many of which would be sublimable, freely soluble in a range of organic solvents, air-, light-, and thermally-stable, and powerful electron acceptors available for use in fundamental studies of the correlations between molecular composition/structure and physicochemical properties. Once the syntheses are scaled up, these compounds will also be available for applications such as molecular transistors, photovoltaics, ferroelectrics, non-volatile memory, non-

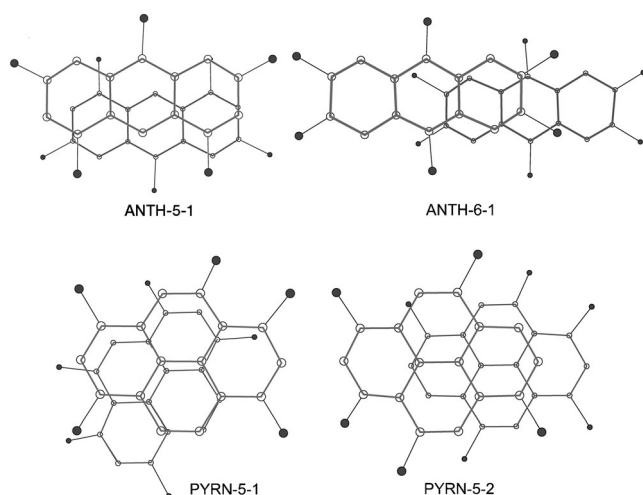


Figure 3. Comparison of portions of the X-ray structures of ANTH-5-1 and ANTH-6-1 (top) and PYRN-5-1 and PYRN-5-2 (bottom). Both F and H atoms have been omitted for clarity, and the C atoms are shown as spheres of arbitrary size (see the Supporting Information for thermal ellipsoid plots). The C atoms of the CF₃ groups shaded gray. Each drawing is oriented so that the least-squares plane of the lower aromatic core is in the plane of the page. For ANTH-5-1, ANTH-6-1, and PYRN-5-2 the least-squares planes of the upper aromatic cores are rigorously parallel to the planes of the lower cores. For PYRN-5-1, the least-squares plane of the upper aromatic core is tilted 5.2° with respect to the plane of the lower core.

linear optics, fluorescent probes, pharmaceuticals, agrochemicals, organometallic catalysts, and composite polymer/PAH blends.

Received: January 6, 2013
Revised: January 31, 2013
Published online: March 25, 2013

Keywords: electrochemistry · electron affinity · polycyclic aromatic hydrocarbons · synthetic methods · trifluoromethylation

- [1] a) M. L. Tang, Z. A. Bao, *Chem. Mater.* **2011**, *23*, 446–455; b) M. H. Yoon, A. Facchetti, C. E. Stern, T. J. Marks, *J. Am. Chem. Soc.* **2006**, *128*, 5792–5801; c) F. Babudri, G. M. Farinola, F. Naso, R. Ragni, *Chem. Commun.* **2007**, 1003–1022; d) J. E.

Anthony, A. Facchetti, M. Heeney, S. R. Marder, X. W. Zhan, *Adv. Mater.* **2010**, *22*, 3876–3892; e) H. R. Sun, A. Putta, M. Billion, *J. Phys. Chem. A* **2012**, *116*, 8015–8022.

- [2] H. Usta, A. Facchetti, T. J. Marks, *Acc. Chem. Res.* **2011**, *44*, 501–510.
[3] Y. C. Chang, M. Y. Kuo, C. P. Chen, H. F. Lu, I. Chao, *J. Phys. Chem. C* **2010**, *114*, 11595–11601.
[4] a) J. Yang, Y. Li, H. Gu, Y. Chen, US Patent, 7,390,901, **2008**; b) M. Schlosser, *Angew. Chem.* **2006**, *118*, 5558–5572; *Angew. Chem. Int. Ed.* **2006**, *45*, 5432–5446; c) S. Geib, S. C. Martens, U. Zschieschang, F. Lombeck, H. Wadeh, H. Klauk, L. H. Gade, *J. Org. Chem.* **2012**, *77*, 6107–6116.
[5] a) O. A. Tomashenko, V. V. Grushin, *Chem. Rev.* **2011**, *111*, 4475–4521; b) E. J. Cho, T. D. Senecal, T. Kinzel, Y. Zhang, D. A. Watson, S. L. Buchwald, *Science* **2010**, *328*, 1679–1681; c) R. N. Loy, M. S. Sanford, *Org. Lett.* **2011**, *13*, 2548–2551; d) Z. Yuan, J. Li, Y. Xiao, Z. Li, X. Qian, *J. Org. Chem.* **2010**, *75*, 3007–3016; e) H. Sun, U. K. Tottempudi, J. D. Mottishaw, P. N. Basa, A. Putta, A. G. Sykes, *Cryst. Growth Des.* **2012**, *12*, 5655–5662; f) S. Miao, A. L. Appleton, N. Berger, S. Barlow, S. R. Marder, K. I. Hardcastle, U. H. F. Bunz, *Chem. Eur. J.* **2009**, *15*, 4990–4993; g) O. Tverskoy, F. Rominger, A. Peters, H. J. Himmel, U. H. F. Bunz, *Angew. Chem.* **2011**, *123*, 3619–3622; *Angew. Chem. Int. Ed.* **2011**, *50*, 3557–3560.
[6] a) G. V. D. Tiers, *J. Am. Chem. Soc.* **1960**, *82*, 5513–5513; b) A. B. Cowell, C. Tamborski, *J. Fluorine Chem.* **1981**, *17*, 345–356; c) A. Bravo, H. R. Bjorsvik, F. Fontana, L. Liguori, A. Mele, F. Minisci, *J. Org. Chem.* **1997**, *62*, 7128–7136.
[7] I. V. Kuvychko, S. N. Spisak, Y. S. Chen, A. A. Popov, M. A. Petrukhina, S. H. Strauss, O. V. Boltalina, *Angew. Chem.* **2012**, *124*, 5023–5026; *Angew. Chem. Int. Ed.* **2012**, *51*, 4939–4942.
[8] X. B. Wang, L. S. Wang, *Rev. Sci. Instrum.* **2008**, *79*, 073108.
[9] J. E. Bartmess in *NIST Chemistry WebBook, NIST Standard Reference Database Number 69* (Eds.: P. J. Linstrom, W. G. Mallard), National Institute of Standards and Technology, Gaithersburg, MD (retrieved November 16, 2012).
[10] R. S. Ruoff, K. M. Kadish, P. Boulas, E. C. M. Chen, *J. Phys. Chem.* **1995**, *99*, 8843–8850.
[11] M. D. Curtis, J. Cao, J. W. Kampf, *J. Am. Chem. Soc.* **2004**, *126*, 4318–4328.
[12] X-ray structures of seven compounds were obtained and have been deposited with the Cambridge Crystallographic Data Centre and three other structures are preliminary X-ray structures have been determined. CCDC 908497 (ANTH-5-1), 908503 (PYRN-5-1), 908499 (PERY-4-1), 908500 (PERY-5-1), 908501 (PERY-6-1), 908502 (PHEN-5-1), and 908504 (TRPH-6-1) contain the supplementary crystallographic data for this paper. These data can be obtained free of charge from The Cambridge Crystallographic Data Centre via www.ccdc.cam.ac.uk/data_request/cif.